The Rotary Magnetostrictive Motor: a Promising Solution for Low Power Actuators

Alexandru Dalea*, Mircea Ignat**, Sorin Deleanu#, Mihai Iordache*, Neculai Galan*

* "POLITEHNICA" University of Bucharest/ Faculty of Electrical Engineering, Bucharest, ROMANIA,
E-mail: alexandru.dalea@upb.ro , mihai.iordache@upb.ro, galannicolae@yahoo.com
** National Institute for Electrotechnics (ICPE), Bucharest, ROMANIA, E-mail: mircea.ignat@icpe-ca.ro
# Northern Alberta Institute of Technology (NAIT), Edmonton, CANADA, E-mail: sorind@nait.ca

***Abstract* – This paper contains a theoretical and experimental study on rotary magnetostrictive motor, performed with the purpose of determining the optimal conditions of operation. The two main types of magnetostrictive motors known from the literature, inchworm respectively resonance present the advantage of large and accurately controlled developed torques for low speed values. The electromagnetic torque developed by the rotary magnetostrictive motor being proportional to the frequency of the current circulating through its inductor, became the subject of frequency control methods. This fact lead to the idea of controlling the torque by controlling the frequency of the current, with direct implication in the domain of torque-controlled drives. Although the actuator represents the central part of any magnetostrictive device, the entire magnetic circuit configuration determines the position of the permanent magnet operating point on the linear portion of the magnetostrictive characteristic. The paper includes two different methods, applied for the permanent magnet operating point allocation. The magnetostrictive torque was determined and expressed as function of time, for the full cycle of the periodical current carried by the actuator's coil. The cycle of the magnetostrictive torque is identical with the cycle of the periodical current circulating through the coil of the actuator. The analytical mathematical model developed and presented in the paper considers both regimes, starting and running, making possible the tracking of the operation point. Furthermore, was possible to determine the moment of separation between the rotor disk and the flexible friction element. Several acquired data, recorded at different values of power supply frequency, demonstrate a good correlation between the theory and experiment.**

Cuvinte cheie: *motor magnetostrictiv rotativ, actuator, magnet permanent, cuplu magnetostrictiv, funcționare optimă.*

Keywords: *rotary magnetostrictive motor, actuator, permanent magnet, magnetostrictive torque, optimal operation.*

I. Introduction

The magnetostrictive effect is defined by the elongation or contraction associated with the spontaneous magnetization of a magnetostrictive material of a quasi-linear (bar) shape. In the presence of a gradually increasing magnetic field *H*, the length of the magnetostrictive material increases as well up to a saturation value. Some magnetostrictive actuators possess displacement capabilities along both axial and radial directions, with direct application in machine tools [1]. This type of actuator ensures a very high precision of operation, accurately controlling the position on a plane surface. There are several other application examples of magnetostrictive motor, described in [2], built either as linear or rotary. Generally, the inductor consists of a Terfenol made bar, introduced inside of an inductor whose turns surround it. Energizing the inductor with alternating current, will results in the expansion-contraction movement of the bar: this is the simplest magnetostrictive motor with linear displacement. Obviously, the conversion of the linear displacement into a revolving one is possible [1-6]. Several electric drive solutions based on magnetostrictive motors (i.e. linear, rotational or stepper), share a common characteristic: the rotational movement generated utilizing several linear actuators [7-35]. Recent became available a magnetostrictive motor type capable to perform axial and radial movements [13]. This motor offers a clear solution for the position control in a plain area, using two directions (i.e. two degree of freedom or 2-DOF), with direct application in high precision machining. Terfenol-D is the ideal material used in magnetostrictive motors fabrication and presents remarkable characteristics: high magnetic stress of 1000-2000 ppm for a magnetic field of 50 – 200 kA/m in volumetric materials, largest temperature range for operation and an acceptable compromise between high tension and high Curie temperature [20-26]. Giant magnetostrictive actuators (GMA) manufactured using giant magnetostrictive materials (GMM) qualify as a special category [21-23], characterized by high Curie temperatures, large developed stress, and a large displacement in comparison with the piezoelectric materials. GMM can provide noncontact driving without electrodes, whereas the fabrication process is relatively simple for a multitude shapes [24]. Adding a relatively inexpensive fabrication to the features presented above, made the GMA suitable for many applications, like electro hydraulic servo valves [15], high pressure common rail injectors [22, 23], rotary-linear motion, ultraprecise fabrication operations [24], active vibration control [29], etc. Addressing the local power consumption, as a critical factor [28], a solution resulted in a complete three-phase actuator kit including the power electronic converter and the DSP based control unit, in which the magnetostrictive motor shaft position is monitored by a laser-based position sensor, and the displacement is controlled by a closed loop system. Such a system has remarkable capabilities like a high force of 410N, a speed up to 60mm/min and a displacement of 45mm. The power consumption recorded during the tests was only 95W, whereas the actuator has the capability of self-braking, being able to preserve its position if the power is cut-off. This paper analyzed certain considerations regarding the development of the magnetostrictive torque developed by the rotary magnetostrictive motor, together with the requirements aiming for op-

Note: This paper is an extended version of "Optimal Operation of Rotary Magnetostrictive Motor," presented at "2018 International Conference on Applied and Theoretical Electricity (ICATE)", Craiova, Romania, October 4 – 6, 2018.

timal operation conditions and high performance. The dependency between the magnetostrictive torque and frequency of the current is determined and completed with mechanical characteristic. The theoretical solution given in this paper states the condition for high performance operation of the actuator: the permanent magnet must operate at a certain value of the magnetic field strength. This value corresponds to the middle of the linear portion of "elongation-magnetic field" characteristic, precisely defined for the utilized magnetostrictive material. This study targeted multiple objectives concerning the magnetostrictive motor: developed torque analysis, mechanical characteristic and the comparison between the theoretical and experimental results. A rotary magnetostrictive motor-built prototype was the subject of laboratory tests for comparing theoretical data with experimental ones.

II. MAGNETOSTRICTIVE MOTOR

Magnetostrictive motors are of three main types: linear motors, rotary motor and pulsating motors. However, the utilized actuators have similar constructive configurations [5-7]. The principal components of the rotary magnetostrictive motor are the actuator and the mobile disk, placed on a vertical shaft and guided by two bearings (see Fig. 1, and for operation details Fig. 2). The current i_b circulating through the coil of the actuator is (1):

$$i_b = I\sqrt{2}\,\sin\omega t \tag{1}$$

The magnetomotive force associated to the alternating, sinusoidal current described by equation (1), generates an alternating magnetic field as well (2):

$$H_b = H_{bm}\,\sin\omega t \tag{2}$$

The characteristic of the magnetostrictive element given in Fig. 3 represents the dependency between the elongation ΔL and the strength of the magnetic field H. The linear portion of the characteristic from expressed by equation (3), is:

$$\Delta L = \lambda_M H \tag{3}$$

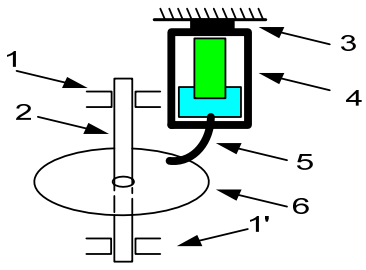

Fig. 1.The "generic" sketch of the rotary magnetostrictive motor : 1 şi 1' – bearings, 2 – shaft, 3 – console, 4 –actuator, 5–friction element, 6 – rotor

Applying Hooke's Law, results dependency between the elongation and the effort according to equation (4):

$$\Delta L = \lambda_H F \tag{4}$$

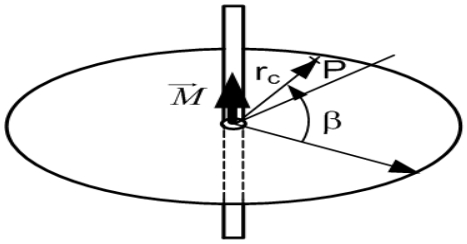

Fig. 2.The rotor's disk: P – contact point between the disk and the friction element, r_c – the radius of the circle containing the point of contact P, β – the angle which denotes the position of point P, M-the developed torque which is applied to the rotor

The result is the effort as a function of t and the coil's current i_b. During the time interval of elongation ΔL, the friction element 5 is in contact with the disk, and the disk starts rotating (see Fig. 1 and Fig. 2). Conversely, during the contraction interval, ΔL and the friction element does not touch the disk until ΔL becomes equal to zero. The process is repetitive. The idealized characteristic (i.e. linearized for intervals) approximates the time variation of the developed torque M presented in Fig. 4 [6-12].

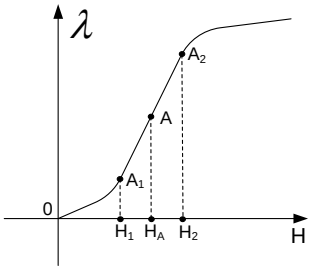

Fig. 3.The Magnetostrictive characteristic for the material (Terfenol D or GalFeNol)

The torque M applied to the disk is directly proptional to the effort F and defined by the equation (5):

$$M = F\,r_c\cos\alpha_0 = \frac{\Delta L}{\lambda_h} r_c\cos\alpha_0 \tag{5}$$

The term r_c represents the radius of the fictitious circle containing the point of contact and centered in the center of cross-section of the mobile disk's shaft, α_0 is the angle between the vector representing the effort F applied to the actuator and the horizontal of the disk.

A. Trapezoidal Torque Model

For a full cycle T, (6) define the developed torque.

$$M(t) = \begin{cases} at, t \in \left[0, \dfrac{T}{3}\right] \\ 1, t \in \left[\dfrac{T}{3}, \dfrac{5T}{6}\right] \\ 0, t \in \left[\dfrac{5T}{6}, T\right] \end{cases} \tag{6}$$

Because the torque has a periodical time variation, a reduced Fourier series of sine functions is necessary to express it (7):

$$M(t) = M_0 + \sum_{k=1}^{\infty} C_{km} \sin(k\omega t + \alpha_k) \tag{7}$$

The term M_0 represents the average value of the magnetostrictive torque and is practically responsible for the energy conversion from magnetic into mechanical. The terms present in the infinite series are torque harmonics. For steady state, these harmonics have no contribution to the energy conversion. In the equation (8), one can remark the equivalence between the work performed by the magnetostrictive and the work performed by the mobile disk. The equality is valid for the reference frequency f_0 as well as for any frequency f from the domain of interest. The torque is frequency dependent (see Fig. 5).

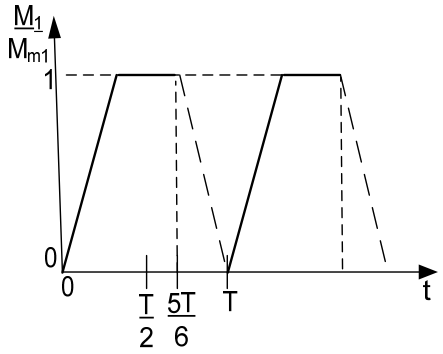

Fig. 4.The time variation of the magnetostrictive torque M

$$L_{M0} = \int_0^{\Delta L(T_0)} F_1(t)\, d(\Delta L) = \int_0^{\beta(T_0)} M_1(t)\, d\beta \qquad 1$$
$$L_M = \int_0^{\Delta L(T_0)} F_f(f)\, d(\Delta L) = \int_0^{\beta(T_0)} M_1(f)\, d\beta \tag{8}$$

Notations are consistent with Fig. 5. There is no expression linking the rotational speed to the frequency available in the mathematical model (8). However, one can determine a torque – frequency dependency. Considering the inductor current i_b at the frequencies f_0 (reference frequency) and f (any frequency from the domain of interest), the torque – frequency function appears in Fig. 5.

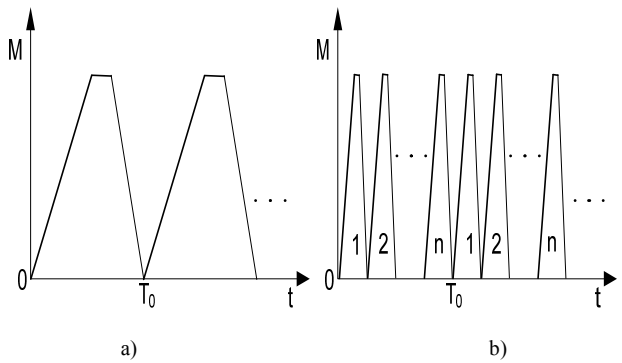

a) b)

Fig. 5. a) The torque M represented as time dependent at frequency $f_0 = 1$ and a cycle with duration T_0 and b) The torque M represented as time dependent at frequency $f = nf_0$ and a cycle with duration $T = T_0/n$.

The following equations described in (9) are valid:

$$\int_0^{\Delta L(T_0)} F_f(f) d(\Delta L) = \int_0^{\Delta L(T_1)} F_f(f) d(\Delta L) + \int_0^{\Delta L(T_2)} F_f(f) d(\Delta L) +$$
$$+ \int_0^{\Delta L(T_n)} F_f(f) d(\Delta L); \quad T_1 = T_2 = \ldots = T_n = \frac{T_0}{n}$$
$$\Rightarrow \int_0^{\Delta L(T_1)} F_f(f) d(\Delta L) = \int_0^{\Delta L(T_2)} F_f(f) d(\Delta L) =$$
$$= \int_0^{\Delta L(T_n)} F_f(f) d(\Delta L) = \int_0^{\Delta L(T_0/n)} F_f(f) d(\Delta L)$$
$$\int_0^{\beta(T_0)} M_f(f) d\beta = \int_0^{\beta(T_1)} M_f(f) d\beta + \int_0^{\beta(T_2)} M_f(f) d\beta + \tag{9}$$
$$+ \int_0^{\beta(T_n)} M_f(f) d\beta =$$
$$= n \int_0^{\beta(T_0/n)} M_f(f)\, d\beta = n \int_0^{\beta(T_0)} M_1(t)\, d\beta \Rightarrow$$
$$\Rightarrow \int_0^{\beta(T_0)} M_f(f)\, d\beta = n \int_0^{\beta(T_0)} M_1(t)\, d\beta$$

All the calculations from (9), performed for the duration of a full cycle T_0 correspond to reference frequency f_0 and they count on the properties (10a, b) of defined integrals.

$$\int_a^{a+b} f(x)dx = \int_0^b f(x)dx = F(b) - F(0) \tag{10a}$$

$$\int_a^b f(x)dx = \int_{a/k}^{b/k} f(k\,x)dx = F(b) - F(a) \tag{10b}$$

From the final form of the equation (9), one can deduce relationship (11) as dependency between the magnetostrictive torque M_f developed at frequency f and the torque M_1 developed at the reference frequency $f_0 = 1\ Hz$.

$$M_f = f\, M_1 \tag{11}$$

According to (11) the torque M_f developed for any frequency of the inductor current is proportional to the frequency. This proportionality between the developed torque and frequency is consistent for any type time variation of the torque within a cycle, if the variation is the same within every cycle of operation. The rotor dynamics given by the system (12a-d) is:

$$J\frac{d\Omega}{dt} = J\frac{\pi}{30}\frac{dn}{dt} = M_a - M_r \tag{12,a}$$
$$M_a = k_v M_f \tag{12,b}$$
$$M_r = M_D + M_s \tag{12,c}$$
$$M_D = D\Omega \tag{12,d}$$

In the equations (12a-d), the resultant torque opposed to the rotation M_r is composed from a true load torque M_s (main component) and some additional components like friction and parasitic torques. The following notations

clarify the equations (12a-d). J is the moment of inertia of the mobile part. M_D represents the torque due to viscosity of the bearings. M_s – the true load torque required by the driven mechanism; M_a – the active (driving) torque (i.e. the average value of M_0, whereas neglecting the harmonics, according to (7)), and k_v is a factor used for calculating the average value of the developed torque. The mechanical characteristic of the rotary magnetostrictive motor namely $n = f(M_s)$, resulted directly from the equation (12a). In conditions of operating at steady state characterized by constant angular speed Ω=const. and constant load torque M_s = const. and in presence of viscosity in the bearings $D \neq 0$ is obtained:

$$\Omega = ct.; \quad \Rightarrow \Omega = \frac{\pi n}{30} = \frac{M_a - M_s}{D} \Rightarrow$$
$$\Rightarrow n = \frac{30}{\pi} \frac{fk_v M_1 - M_s}{D} \tag{13}$$

If the viscosity of the bearings is negligible, then $D = 0$ and the load torque is dependent upon the angular speed with a relationship $M_s = K\Omega$, is found that:

$$\Omega = ct.; \quad \Rightarrow M_a - M_r = 0 \Rightarrow$$
$$\Rightarrow \Omega^n = \left(\frac{\pi n}{30}\right)^n = \frac{M_a}{K} \Rightarrow \tag{14}$$
$$\Rightarrow n = \frac{30}{\pi} \sqrt[n]{\frac{fk_v M_{f_s}}{K}}$$

The 2 cases mentioned by (13) and (14) confirm that the rotational speed is frequency dependent. The equations detailing this dependency are different and determined by how each of the terms the opposed torque M_r depends upon the angular speed Ω (or rotational speed n).

B. Sinusoidal Torque Model

The torque has a similar time variation as the elongation (see Fig. 6).

$$\frac{M}{M_m} = \begin{cases} \frac{1}{2}(1 - \cos \omega t), \omega t \in \left[0, \quad \frac{7\pi}{6}\right] \\ 0, \omega t \in \left[\frac{7\pi}{6}, \quad 2\pi\right] \end{cases} \tag{15}$$

Such a periodical function, decomposed in Fourier series appears in (16).

$$M(t) = M_0 + \sum_{k=1}^{\infty} M_{km} \cos(k\omega t + \alpha_k). \tag{16}$$

It is convenient to consider the maximum value of the function $M(t)$ equal to 1. Therefore, the results following simulation can pe peroperly extrapolated. M_0 represents the average value $M(t)$, whereas M_{km}, respectively α_k are the magnitudes and the phase angles of the harmonics of the Fourier decomposition (16). The rotational motion equation written at constant angular speed is (17):

$$J\frac{d\Omega}{dt} = J\frac{\pi}{30}\frac{dn}{dt} = M(t) = M_0 + \sum_{k=1}^{\infty} M_{km} cos(k\omega t + \alpha_k) \tag{17}$$
$$\Rightarrow n = \frac{30}{J\pi} M_0 t + \frac{30}{J\pi} \sum_{k=1}^{\infty} \frac{M_{km}}{k\omega} sin(k\omega t + \alpha_k),$$

The term J is the moment of inertia of the system in rotational motion. Analyzing equation (16), one can remark that for such a torque, the magnetostrictive motor cannot operate unloaded, whereas the rotational speed increases linearly in time. This fact id due to the lack of correlation between the value M_0 and the rotational speed n. Consequently, the mechanical characteristic may not be precisely defined for certain values of the load torque M_s.

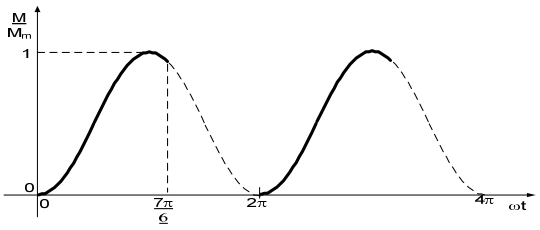

Fig. 6. Torque M_a represented as a periodical function of time.

III. Efficient Energy Conversion

For analyzing the process of energy conversion, one can consider to start from the magnetostrictive characteristic, defined as the absolute elongation ΔL (or per unit one $\lambda = \Delta L/L$) of the specified material as a function of the applied magnetic field strength H (see Fig. 3). There are three points of interest on the linear (A_1A_2) section of the magnetostrictive characteristic, marked as A_1, A, A_2. The point A represents the half of the linear section on the magnetostrictive characteristic. The efficiency evaluation of the entire energy conversion requires measuring or estimating the mechanical work consumed during the operation by the actuator. Within the linear section of the magnetostrictive characteristic, the elementary mechanical work corresponding to a single elongation is (18):

$$\delta L_M = F\, d(\Delta L) = \frac{\Delta L}{\lambda_H} d(\Delta L) \Rightarrow$$
$$\Rightarrow L_M = \frac{1}{\lambda_H} \int_0^{\Delta L} \Delta L\, d(\Delta L) = \quad \frac{\Delta L^2}{\lambda_H} = \frac{\lambda^2}{\lambda_H L^2} \tag{18}$$

The equation (18) emphasizes the strong dependency of the work L_m on the square of the elongation ΔL. A large elongation is the main requirement requested by an efficient energy conversion. Due to the alternating nature of the inductor current i_b, both alternations of the magnetic field must be kept within the linear portion of the magnetostrictive characteristic. This condition shows a need for accurate determination of the point A through calculations followed by confirmation through adequate experiments. This condition imposes the utilization of the linear por-

tion of the magnetostrictive characteristic to its entire extent.

A. Magnetic Permeances of the Actuator

Fig. 7 displays a cross-section view of the actuator and its principal constructive elements. Because the permanent magnet strongly influences the actuator's performance, the determination of the "operation point" on the magnetic characteristic is of great interest. The main characteristics of a permanent magnet are the demagnetizing characteristic and its geometry. To associate an equivalent magnetic circuit to a permanent magnet is a challenging task [1-4, 7-9]. The demagnetizing characteristic belongs to the second quadrant of the *B-H* ($B \geq 0$, $H \leq 0$) plane, where B_r is the residual flux density and H_c is the intensity of the coercive magnetic field (see Fig. 8).

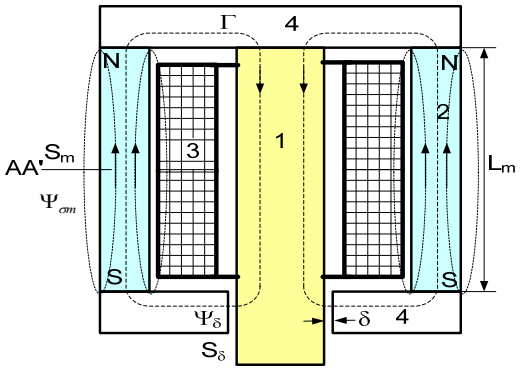

Fig. 7. Actuator construction (vertical cross-section): 1- rod made of terfenol; 2 – permanent magnet; 3 –inductor; 4 – ferromagnetic flanges

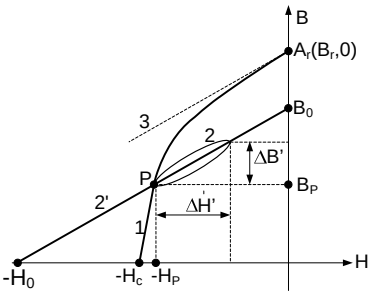

Fig.8. 1 – demagnetizing curve; 2 – returning curve; 2'- returning line; 3 – tangent line to demagnetizing curve at the point A_r

Analyzing Fig. 8, let us assume that the operation point of actuator's permanent magnet is *P*. If the magnetic flux density increases, the operating point *P* will follow the curve *2* instead of characteristic *1*, drawing a local, narrow hysteresis cycle. The straight line *2'*, named restoring line, approximates this local hysteresis cycle. The intersections of the restoring line with the horizontal, respectively vertical axes determine the values $-H_0$ on the axis of the magnetic field strength, respectively B_0 on the axis of the magnetic flux density. Whereas a permanent magnet belongs to a magnetic circuit, has three characteristics: magnetomotive force Θ_0, leakage reluctance $R_{m\sigma}$ and the reluctance R_m of the magnetizing flux path along the permanent magnet (see Fig. 7 and Fig. 8 for notations).

$$\Theta_0 = H_0 L_m \tag{19}$$

$$R_m = L_m / (\mu_m S_m) \tag{20}$$

When excited with current i_b, the inductor (see Fig. 7, component 3) produces a magnetic field, which is interacting with the magnetic field produced by the permanent magnet. Despite the sinusoidal time variation of the magnetic flux density $B(t)$, the magnetic field strength $H(t)$ is not. This fact is due to hysteresis. The magnetic field strength $H(t)$ can be decomposed using Fourier series, keeping only the fundamental harmonic, namely $H_1(t)$. The fundamental harmonic $H_1(t)$ leads $B(t)$ with an angle γ_1.

$$\begin{aligned} &H_1(t) = H_{m1} \sin \omega t\,; \\ &B_1 = B_1(t) = B_{m1} \sin(\omega t - \gamma_1) = \\ &= B_1' + B_1'' = B_{m1}' \sin \omega t + B_{m1}'' \cos \omega t \end{aligned} \tag{21,a}$$

$$B_{m1}' = B_{m1} \cos \gamma_1\,;\; B_{m1}'' = -B_{m1} \sin \gamma_1 \tag{21,b}$$

$$\mu = \frac{B_{m1}}{H_{m1}} \tag{21,c}$$

$$\mu' = \mu_0 \mu_r' = \frac{B_{m1}'}{H_{m1}} = \mu \cos \gamma_1 \tag{21,d}$$

$$\mu'' = \mu_0 \mu_r'' = \frac{B_{m1}''}{H_{m1}} = \mu \sin \gamma_1 \tag{21,e}$$

Sinusoidal variables B_1 and H_1 converted into complex form appear in equations (22). In this way, one can introduce the complex permeability $\underline{\mu}$ as subsequent:

$$\underline{H}_1 = H_{m1} e^{j\omega t} \tag{22,a}$$

$$\underline{B}_1 = B_{m1} e^{j(\omega t - \lambda_1)} \tag{22,b}$$

$$\underline{\mu} = \frac{\underline{B}_1}{\underline{H}_1} = \mu e^{-j\gamma_1} = \mu' - j\mu'' \tag{22,c}$$

Removing the time from the equations (21), one can obtain the equations (23), after brief calculations:

$$B_1 = \mu' H_1 \pm \mu'' \sqrt{H_{m1}^2 - H_1^2} \tag{23,a}$$

$$B_1' = \mu' H_1 \tag{23,b}$$

$$B_1'' = \pm \mu'' \sqrt{H_{m1}^2 - H_1^2} \tag{23,c}$$

The hysteresis cycle of a magnetic material can be decomposed according to (22) into two components.
There are two different relationships (22, b, c) between magnetic flux density and magnetic field strength. The component B'_1 corresponds to reversible magnetizing processes, while B''_1 corresponds to the irreversible magnetizing ones. The latter is an ellipse with axes overlap-

ping the axes of coordinates (see Fig. 9). The description of the ellipse relies in the following equations (24):

$$B_1'' = \pm\mu''\sqrt{H_{m1}^2 - H_1^2} \Rightarrow$$
$$\left(\frac{\mu_0 H_1}{\mu_0 H_{m1}}\right)^2 + \left(\frac{B_1''}{\mu'' H_{m1}}\right)^2 = 1 \qquad (24,a)$$

$$tg\alpha' = \mu_r' \qquad (24,b)$$

$$tg\alpha'' = \mu_r'' \qquad (24,c)$$

From equations (24), one can determine the relative permeability μ_r' and μ_r'' (see Fig. 9).

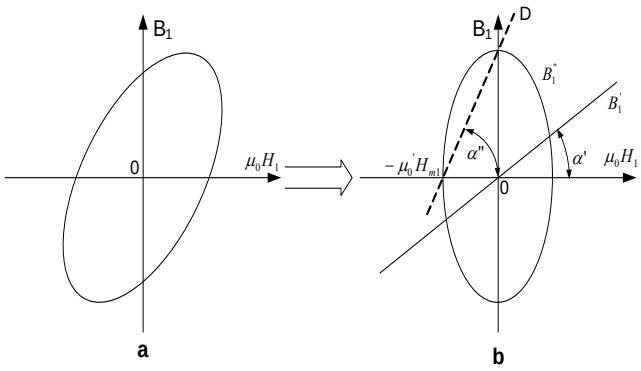

Fig.9. a) "Ellipse shaped" hysteresis cycle and its components; b) Complex permeability representation.

The real part of the complex permeability is equal to the slope of the line $B_1=\mu' H_1$. The ellipse (see Fig. 9) intersects the rectangular axes of coordinates in two points. A straight line joining the two points (- $\mu_0 H_{m1}$, 0), (0, $\mu'' H_{m1}$) has slope equal to μ''. The specific hysteresis loss (W/m^2), for an elliptic shaped cycle p_H calculated at frequency f is:

$$p_{Hi} = \pi f H_{m1i} B_{m1i} \sin\gamma_1 \qquad (25)$$

The complex magnetic reluctance of an element with the length l_i and cross-section S_i expressed (26), is:

$$\underline{R}_M = R_c + j R_d = \frac{l_i}{S_i \underline{\mu}} = \frac{l_i}{S_i \mu^2}\left(\mu' - j\mu''\right) \qquad (26,a)$$

$$R_c = \frac{l_i \mu'}{S_i \mu^2} = \frac{l_i \mu' H_{m1}}{H_{m1} S_i \mu^2} = \frac{\mu' l_i H_{m1}}{\mu \Phi_i}\cos\gamma_1 \qquad (26,b)$$

$$R_d = \frac{l_i \mu''}{S_i \mu^2} = \frac{l_i \mu''}{S_i \mu^2}\frac{P_H}{(S_i l_i)\pi f H_{m1} B_{m1}\sin\gamma_1} = \frac{2P_{Hi}}{\omega\Phi_i^2} = \frac{2\, p_H G_{fi}}{\omega\Phi_i^2} \qquad (26,c)$$

$$\Phi_i = H_{m1} S_i \mu \qquad (26,d)$$

$$p_{Hi} = \frac{P_{Hi}}{G_{fi}} \qquad (26,e)$$

Following the decomposition of the hysteresis cycle, the two reluctances calculated with (26) will be referred as "conservative reluctance" (R_c) and "dissipative reluctance" (R_d) [10]. In Fig. 10, one can visualize the equivalent magnetic circuit of the actuator from figure 7.

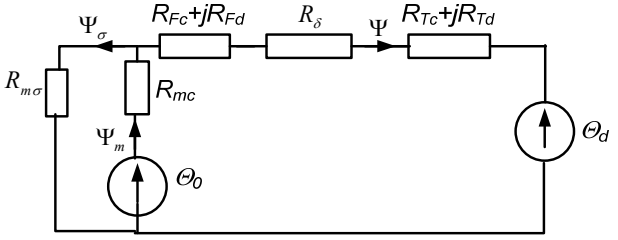

Fig.10. Equivalent magnetic circuit of the actuator (figure 6) including the magnetomotive forces Θ_0 and Θ_d.

The equivalent schematic of a magnetic circuit becomes very useful for the fulfillment of the two outcomes required by the optimal operation of a magnetostrictive motor: the operating point of the permanent magnet, respectively the magnetomotive force of the inductor. The equivalent reluctance of the magnet circuit from Fig. 10, in case of $\Theta_0 \neq 0$ and $\Theta_d = 0$ is (27):

$$R_{e0} = R_{0c} + j R_{0d} = R_{mc} + R_{mo}\cdot K_R \qquad (27,a)$$

$$K_R = \frac{R_{Fc} + R_\delta + R_{Tc} + i\left(R_{Fd} + R_{Td}\right)}{R_{mo} + R_{Fc} + R_\delta + R_{Tc} + i\left(R_{Fd} + R_{Td}\right)} \qquad (27,b)$$

For the case $\Theta_d \neq 0$, and $\Theta_0 = 0$ the equivalent reluctance is (28):

$$R_{eD} = R_{Dc} + j R_{Dd} = R_{Fc} + R_\delta + R_{Tc} + i\left(R_{Fd} + R_{Td}\right) + \frac{R_{mo}\, R_{mc}}{R_{mo} + R_{mc}} \qquad (28)$$

B. Magnetomotive force of the Actuator

The magnetomotive force of the inductor Θ_d must be able to produce a magnetic field of a certain amplitude $\Delta H_m = H_1 - H_{Am}$ (see Fig. 11a), which sweeps the terfenol made rod. From the equivalent magnet circuit one can calculate the magnetomotive force as (29):

$$\Theta_d = wi = R_{eD}\Psi = R_{eD}\mu_F \Delta H S_F \Rightarrow wI_m = R_{eD}\mu_F \Delta H_m S_F \qquad (29)$$

In equation (29), the terms μ_F and S_F are the permeability, respectively the cross-section of the terfenol made bar. The magnetomotive force wI_m depends on power supply and the geometry of the main actuator components (permanent magnet, terfenol rod), This fact drives the calculation of the number of turns w and the maximum current of the inductor I_m. The thermal stress evaluation of the inductor must validate the final solution for the acuator configuration. The inductor must have taps to be

able to modify the magnetomotive force Θ_d (i.e. one for the magnetomotive force given by (29)).

IV. Operating Point of Permanent Magnet

The operating point of the permanent magnet, marked as A_m (see Fig. 11a) on the returning line, gave the opportunity to select the best candidate from the cluster of available permanent magnets. The chosen one must have the closest demagnetizing curve to the theoretically determined returning line. The value of the magnetic field strength H_{Am}, corresponding to the point A_m from the returning line must match the value of the magnetic field strength H_A of the magnetostrictive characteristic (see Fig. 11b), i.e. $H_{Am} = H_A$. The value of the coercive magnetic field strength $|H_c|$ must be large enough. In such a case, the segment P_2P_3 belongs to the confined space bordered by the curve and the axes of coordinates.

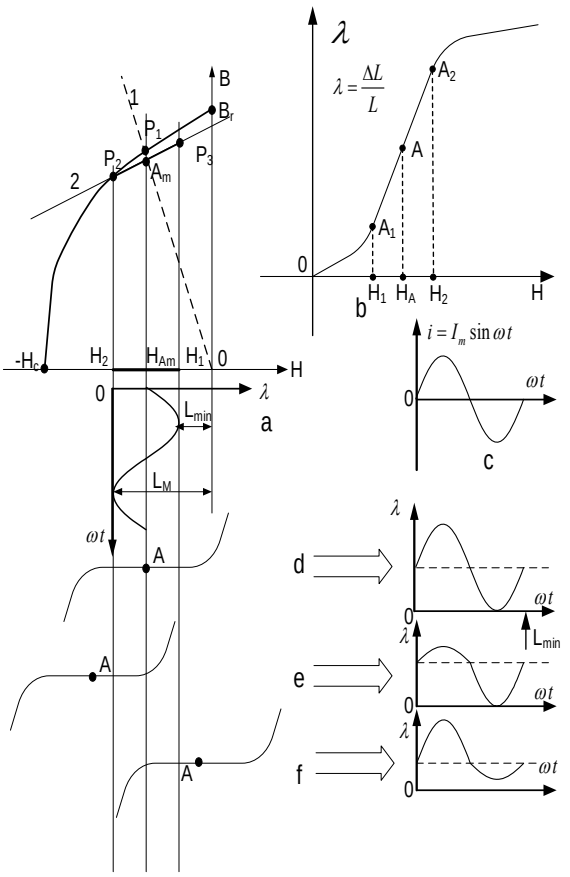

Fig. 11. Coordination between the magnetic field strength values H_{Am} and H_A. a) Examples of positioning for the points A_m and A, 1 – Load characteristic (straight line), 2 – returning line; b) Terfenol Characteristic; c) Time variation of the inductor current; d) Time variation of λ for H_{Am} equal to H_A; e) Time variation of λ for $H_{Am} > H_A$; f) Time variation of λ for $H_{Am} < H_A$.

Three cases represented in Fig. 11d, Fig. 11e and Fig. 11f recommend an experimental procedure to determine the position applied to the points A_m and A. The procedure requires the recording of time variation for the quantityλ, followed by a thorough analysis of the waveform. In the ideal scenario, the value of the magnetic field strength H_{Am} must be the same as H_A. The fine-tuning imposes the presence of an adjustable air gap between the flange and the permanent magnet [10, 11].

V. Simulation Results

All of the performed numerical simulations, according the dynamical rotational motion equation (12), using the afterwards notations, address two particular cases:

Case *a)* (see Fig. 12)

$$\begin{cases} J\dfrac{d\Omega}{dt} = M_a - M_r \Rightarrow J\dfrac{d\Omega}{dt} = kM_f - \left(D\Omega + K\Omega^m\right) \\ M_D = D\Omega, M_S = K\Omega^m \\ m = 2, D = 0.04, K = 0.03, J = 0.015\ kgm^2 \end{cases}$$

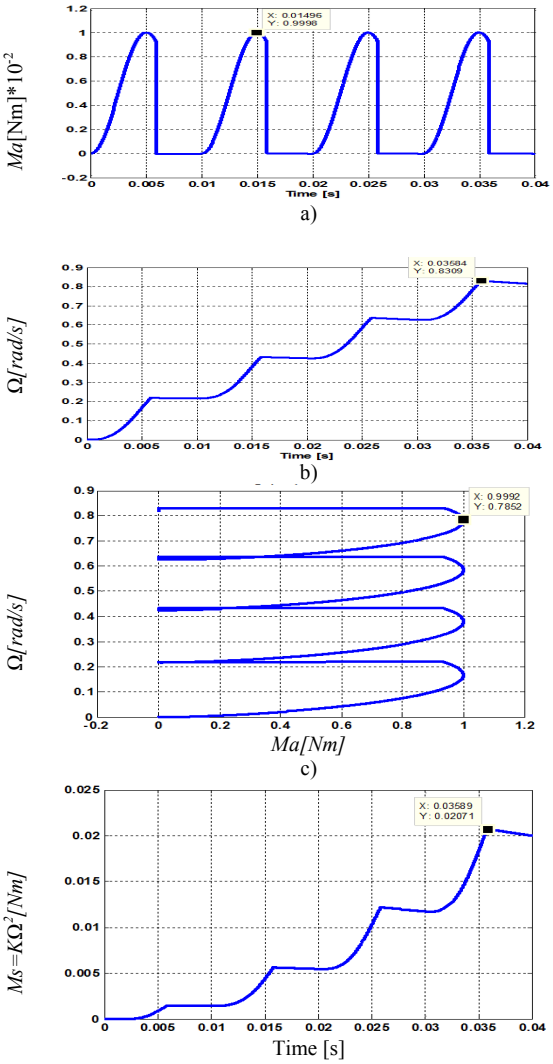

Fig. 12. Simulation results for: $m=2$, $D=0.04$, $k=0.03$, $J=0.015 kgm^2$

Case *b)* (see Fig. 13 and Fig. 14)

$$\begin{cases} J\dfrac{d\Omega}{dt} = M_a - M_r \Rightarrow J\dfrac{d\Omega}{dt} = kM_f - \left(D\Omega + M_S\right) \\ M_D = D\Omega, M_S = \begin{cases} 0, \omega t \in \left[2k\pi, \left(2k\pi + \dfrac{7\pi}{6}\right)\right) \\ 0.5Nm, \omega t \in \left[\left(2k\pi + \dfrac{7\pi}{6}\right), 2(k+1)\pi\right) \end{cases}, \\ m = 2, D = 0.04, K = 0.03, J = 0.045\ kgm^2 \end{cases}$$

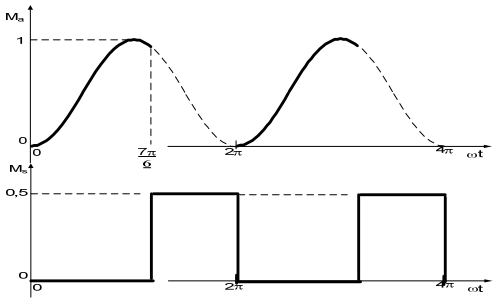

Fig. 13. Developed torque *Ma=Ma(ωt)*, and a step shaped load torque *Ms=Ms(ωt)*

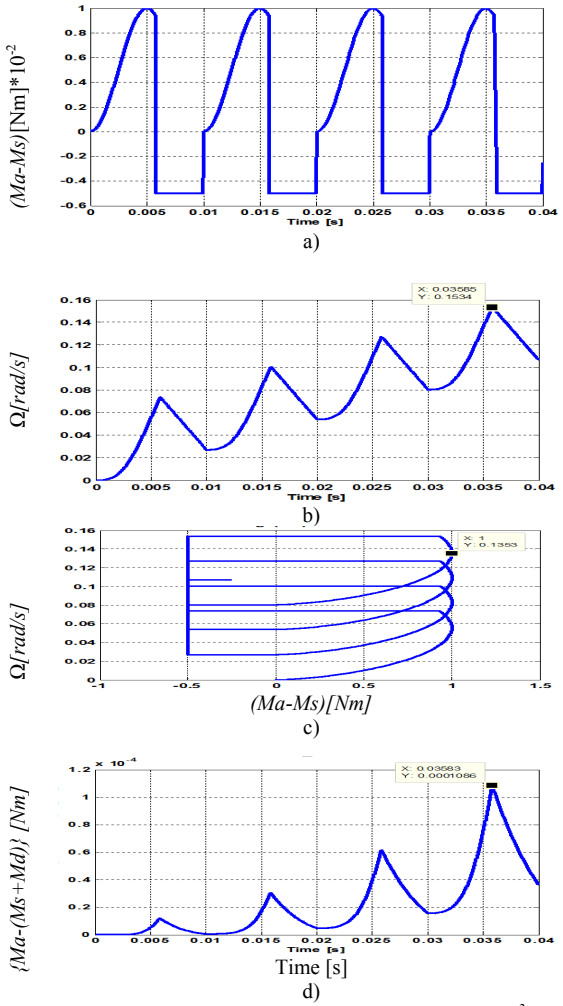

Fig. 14. Simulation results for: *m=2, D=0.04, k=0.03, J=0.045kgm*^{2}

Finite Fourier series decomposition applied to the active torque M_a, true load torque M_s, respectively viscosity torque M_D, delivered the harmonics up to 10th order (see Fig. 15, Fig. 16, and Fig. 17).

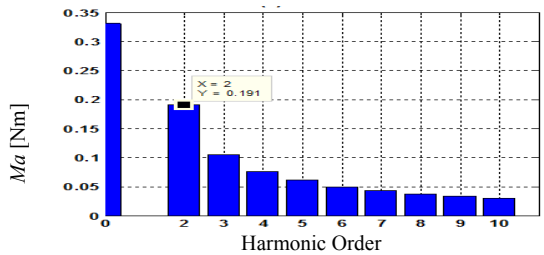

Fig.15. Active Torque Spectrum M_a

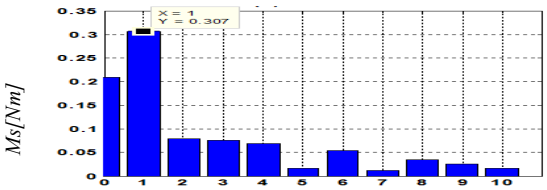

Fig.16. Load Torque M_s

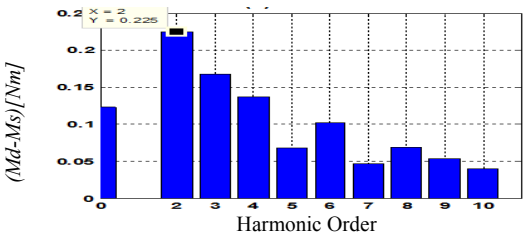

Fig. 17. Difference torque M_a-M_s

Fig. 18, Fig. 19 and Fig. 20 summarize the dependencies between the torques, harmonic and time into surfaces.

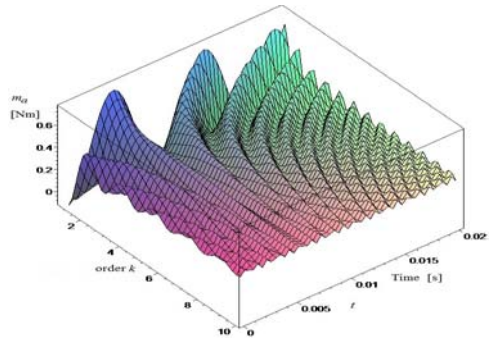

Fig. 18. Active torque magnitude-harmonic-time dependency

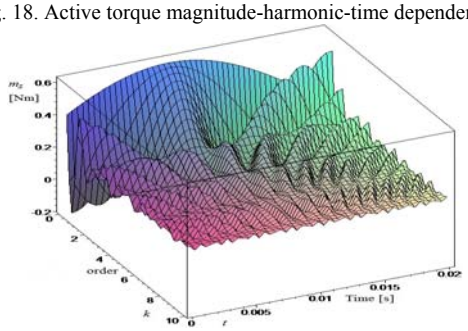

Fig. 19. Load torque magnitude-harmonic-time dependency

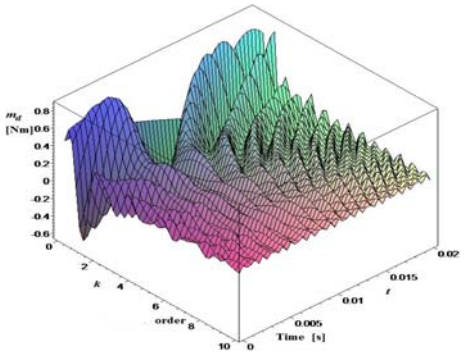

Fig. 20. Difference torque magnitude-harmonic-time dependency

VI. Experimental Results

The experimental tests involved two versions of rotary magnetostrictive motor. In the first configuration of the motor (Fig. 21), the active force is applied on the disk surface.

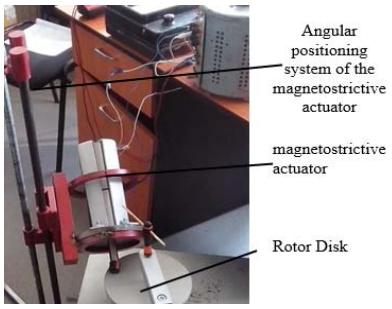

Fig.21.Rotary magnetostrictive motor-first version.

In the second variant, the active force applies to the edge of the disk (Fig. 22).

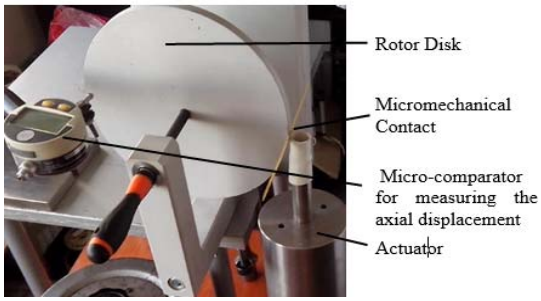

Fig.22. Rotary magnetostrictive motor-second version.

The braking device represents the main difference.

TABLE I. Torque Values

No.	Calculated values versus Measured Values		
	Frequency **[Hz]**	***Calculated Torque*** **[Nm]**	***Measured Torque*** **[Nm]**
1	50	$11.0 \cdot 10^{-3}$	$10.0 \cdot 10^{-3}$
2	80	$17.6 \cdot 10^{-3}$	$15.5 \cdot 10^{-3}$
3	100	$22.0 \cdot 10^{-3}$	$21.3 \cdot 10^{-3}$
4	120	$26.4 \cdot 10^{-3}$	$26.0 \cdot 10^{-3}$
5	150	$33.0 \cdot 10^{-3}$	$30.0 \cdot 10^{-3}$

The experiments followed two objectives: proportionality between the torque and current frequency (confirmed by data from Table I, for an inductor current equal to 2A), and the position of the operating point. Measured values were close to calculations. The operating point of the permanent magnet matched the middle point of the linear portion of the magnetostrictive characteristic. For assessment, the objectives required two independent experiments. The first one required the recording of the time variation of the elongation ΔL. The second experiment required a primary DC energization of the inductor, followed by another one of opposite DC polarity. Measuring at maximum allowed current (thermal considerations) was essential for maximizing the capture of linear portion from the magnetostrictive characteristic (see Table II for data).

TABLE II. Elongantion Versus Current

No.	Measured Values	
	Current **[A]**	***Elongation*** **[µm]**
1	1.10	12.0
2	1.80	18.0
3	2.25	21.0
4	3.00	25.0
5	-1.10	9.8
6	-1.70	17.1
7	-2.18	20.4
8	-3.00	23.8

VII. Conclusions

The actuator represents the most important part in every magnetostrictive type of device, triggering most of research activity towards its design, construction and the operation. Here, a special attention for studying the developed torque emphasized the factors and elements that contribute to performance enhancement. Once estimated, the equivalent magnetic reluctance determined the operating point from the restoring line of permanent magnet. The real hysteresis cycle is equivalent to two fictitious cycles, one drawn by a straight line, the other one by an ellipse. The latter one has its extremities placed on the coordinate axes of the *B-H* plane. From the hysteresis equivalence, two remarkable magnetic reluctances resulted: conservative and dissipative. A performant operation requires a certain magnitude for the magnetic field strength of the permanent magnet. This magnitude must be equal to the magnitude of the magnetic field recorded in the middle of the linear portion of the elongation characteristic of the given magnetostrictive material. Accuracy in calculation of magnetic reluctance is necessary. The dissipative reluctances for the ferromagnetic parts must account, whereas the frequency exceeds certain limits. Following theoretical considerations, the experimental confirmation of the permanent magnet operating point within linear portion of the magnetostrictive characteristic, respectively ΔL - $f(H)$ is necessary. The elongation variation in time, was recorded for a given inductor alternative current, both alternations being assessed against symmetry criteria. If they are symmetrical, one can conclude that the operating point is in the middle of the linear portion of the magnetostrictive characteristic. The other option was to supply the inductor with direct current, followed by direct current of opposite polarity. If the measured elongations of the magnetostrictive material, recorded for both direct current polarities are equal, one can conclude that the operating point is in the middle of the linear portion of the magnetostrictive characteristic. Data tables show a good correspondence between theoretical and experimental results.

Acknowledgment

The authors are grateful to the Department of Micro and Nano Electro-technology within the Romanian National Research Institute for Electrotechnics (ICPE), Bucharest, Romania, for the support regarding the experiments.

Source of research funding in this article: Research program of the Electrical Engineering Department financed by the "POLITEHNICA" University of Bucharest.

Contribution of authors:

First Author – 20%

First coauthor – 20%

Second coauthor– 20%

Third coauthor – 20%

Fourth coauthor – 20%

Received on December 6, 2018

Editorial Approval on December 7, 2018

REFERENCES

[1] C. Kittel, Introducere in Fizica Corpului Solid, Editura Tehnică, Bucureşti, 1972. (in Romanian)

[2] E. Burzo, Fizica fenomenelor magnetice, Ed.Academiei Române, Bucureşti, 1982. (in Romanian)

[3] H. Gavrilă, H. Chiriac, A.Yelon, V. Ionita, Magnetism tehnic şi aplicat Editura Academiei Române, Bucureşti, 2000 (in Romanian)

[4] J.S. Park, O.K. Oh, Y.W. Pamesurerk, N.M. Wereley, "A Novel Concept and Proof of Magnetostrictive Motor," *IEEE Trans. Magn.*, vol. 49, no. 7, pp. 3379 – 3382, 2013.

[5] M. Vranish and D. P. Naik, "Magnetostrictive Direct Drive Rotary Motor Development", NASA Goddard Space Flight Center, Greenbelt, MD 20771.

[6] M. Ignat, I. Puflea, A. L. Cătănescu, A. Vintilă, "Design aspects on the vibration magnetostrictive actuators," XIX International Conference on Electrical Machines – ICEM 2010, Italy, Rome, IEEE Catalog Number: CFP1090B-CDR, Library of Congress: 2009901651, RF-007641 pp. 1-5, 2010,ISBN: 978-1-4244-4175-4.

[7] M. Jufer, Électromécanique, Presses Polytechniques et Universitaires Romandes, Lausanne, 1995.

[8] M. Marinescu, N. Marinescu, "New concepto of permanent magnet excitation for electrical machines: Analytical and numerical computation," *IEEE Trans. Magn*., vol. 28, no. 2, pp. 1390 – 1393, 1992.

[9] A.L. Cătănescu, I. Puflea, M. Ignat, A. Vintilă, "The design aspects on the magnetostrictive actuators", 1st International Workshop „Innovation and Evolution by R&D – SMEs Strategic Partneship", Bucharest, Romania, September 10th-12th, 2009.

[10] A.L. Cătănescu, Acţionări neconvenţionale utilizând actuatori magnetostrictiv, Teză de doctorat, Universitatea "POLITEHNICA" Bucureşti, Romania, 2014. (in Romanian)

[11] M. Ignat, A. L. Cătănescu, I. Puflea, "Applications of the Magnetostrictive Actuators in the Aerospace Structures", International Conference of Aerospace Sciences "AEROSPATIAL 2010", Bucharest, 20-21, October 2010, Proceedings, Section 4. Materials and Structures, ISSN 2067-8622, pp.1-6, 2010.

[12] I.M. Vranish, D.P. Naik, J.B. Restorff, J.P. Teter, "Magnetostrictive direct drive rotary motor development,". *IEEE Trans. on Magn.*, vol.27, no. 6, pp. 5335 – 5357, 1991.

[13] Zhi Li, Xiuyu Zhang, Guo-Ying Gu, Xinkai Chen, and Chun-Yi Su, "A Comprehensive Dynamic Model for Magnetostrictive Actuators Considering Different Input Frequencies With Mechanical Loads," IEEE Transactions on Industrial Information, vol. 12, no . 3, JUNE, pp. 980 – 990, 2016

[14] S. Karunanidhi, M. Singaperumal, "Design, analysis and simulation of magnetostrictive actuator and its application to high dynamic servo valve," Sensors and Actuators A: Physical, vol. 157, pp. 185-197, 2010.

[15] M. Niu, B. Yang, Y. Yang, G. Meng, "Dymanic modelling of magnetostrictive actuator with fully coupled magneto-mechanical effects and various eddy current losses," Sensors and Actuators A: Physical, vol. 258, pp. 163-173, 2017

[16] J. Zhou, Y. Pan, M. Huang, "A novel magnetostrictive drive rotary motor," Solid State Phenomena Vols. 121-123, pp. 1203-1206, 2007. Online available since 2007/Mar/15 at www.scientific.net @ Trans Tech Publications, Switzerland, doi:10.4028/www.scientific.net/SSP.121-123.1203.

[17] Y-W. Park, M. Noh, "Rotary magnetostrictive motor using helical magnetic field," International Journal on Precision Engineering and Manufacturing, vol.17, no.5, pp. 659-663, 2016.

[18] Z. Cao and J. Cai, "Design of a giant magnetostrictive motor driven by elliptical motion," Sensors and Actuators A: Physical, vol. 118, pp. 332-337, 2004.

[19] F. Claeyssen, N. Lhermet, R. Letty, and P. Bouchilloux, "Design and construction of a resonant magnetostrictive motor," IEEE Transactions on Magnetics, vol. 32, pp. 4749-4751, 1996.

[20] A.M, Morega, M. Popa, Mihaela Morega, L. Paslaru-Danescu, "Shape and structure optimization of a magnetostrictive cored actuator," Int. J. of Heat and Technology, vol.34, Special Issue 1, pp.119-124, 2016, http://dx.doi.org/10.18280/ijht.34S115

[21] L. Paslaru-Danescu, A.M. Morega, Mihaela Morega, "A novel magnetostrictive injection actuator based on new giant magnetostrictive material," The 7th International Symposium on Advanced Topics in Electrical Engineering, ATEE 2011,Bucharest, Romania, May 11-14, 2011, IEEE Xplore, ISBN:978-1-4577-0507-6.

[22] G. Xie, P. Zhang, Z.He, D. Li, Z. Yang, Z. Zhao, "Displacement model and driving voltage optimization for a giant magnetostrictive actuator used on a high-pressure common-rail injector," Materials and Design, vol.95, pp.501-509,2016.

[23] G. Xue, P. Zhang, Z. Xue, D. Lin, Y, Huang, W. Xie, "Design and experimental study of a novel giant magnetostrictive actuator," Journal of Magnetism and magnetic materials, vol. 420, pp. 185-191, 2016.

[24] H. Yoshioka, H. Shino, H. Sawano, "A newly developed rotary-linear motion platform with a giant magnetostrictive actuator" CIRP Annals-Manufacturing Technology, vol.62, pp371-374, 2013.

[25] L. Paslaru-Danescu, A.M. Morega, Mihaela Morega, Florentina Numea, P. Marius, Corina-Alice Barbutanu, "A new type of magnetostrictive motor," Electrical Engineering, vol. 99, no.2, pp.610-613, Springer Link, 2017.

[26] W.K Kim, A. Sadighi, "A novel-low power linear magnetostrictive actuator with local three-phase excitation," IEEE/ASME Transactions on Mechatronics, vol.15, no.2, p. 299-307, 2010.

[27] F. Braghin, S. Cinquemani, F. Resta, "A model of magnetostrictive actuators for active vibration control," Sensors and Actuators A: Physical, vol. 165, pp.342-350, 2011.

[28] W. Zhu, L.X. Bian, L. Chung, X.T. Rui, "Nonlinear compensation and displacement control of the bias-rate-dependent hysteresis of a magnetostrictive actuator," Precision Engineering, vol. 50, pp. 107-113, 2017.

[29] R. Joshi, R. Kadoli, "Magneto-mechanical coupled magnetostriction model for Terfenol-D under step input," International Conference on Advances in Manufacturing and Materials Engineering, Procedia Material Science 5, pp.154-163, 2014.

[30] C.C. Hong, "Application of magnetostrictive actuator," Materials and Design, vol. 46, pp. 617-621, 2013.

[31] A.M. Morega, P. Marius, Mihaela Morega, "Optimizarea unui actuator magnetostrictiv (The optimization of a magnetostrictive actuator)," Simpozionul de Masini Electrice, SME-14, University "POLITEHNICA" of Bucharest, Romania, October 3rd, 2014 (in Romanian).

[32] M. Ignat, N. Galan, A. Dalea, "Short Introduction on the magnetostrictive motor," Bulletin of Micro and Nanoelectrotechnologies, no.1-2, pp. 29- 34, 2015

[33] M. Ignat, G. Zarnescu, I. Puflea, Al. Catanescu, L.Paslaru, V. Stoica, "Actuatori electromagnetici (Electromagnetic Actuators),", Ed. Electra, 2008, pp. 22-50 (in Romanian).

[34] J.F. Gieras, M. Wing, "Permanent Magnet Motor Technology. Design and Applications Second Edition. Revised and Expanded," Marcel Dekker, 2002, pp. 50-68.

[35] A. Dalea, M. Ignat, S. Deleanu, M. Iordache, N. Galan, "Optimal Operation of Rotary Magnetostrictive Motor,"2018 International Conference on Applied and Theoretical Electricity (ICATE), Craiova, Romania, October 4 – 6 2018, IEEE Xplore, Electronic ISBN: 978-1-5386-3806-4, DOI:10.1109/ICATE.2018.8551481.